

Characterization of Photocycle Intermediates in Crystalline Photoactive Yellow Protein^{†¶}

Remco Kort^{*1,2}, Raimond B. Ravelli³, Friedrich Schotte^{‡2}, Dominique Bourgeois^{2,4}, Wim Crielaard¹, Klaas J. Hellingwerf¹ and Michael Wulff²

¹Laboratory for Microbiology, Swammerdam Institute for Life Sciences, University of Amsterdam, Amsterdam, The Netherlands;

²European Synchrotron Radiation Facility, Grenoble Cedex, France;

³European Molecular Biology Laboratory Grenoble Outstation, Grenoble Cedex, France and

⁴Laboratoire de Cristallographie et Cristallogénèse des Protéines, UMR 9015, Institut de Biologie Structurale Jean-Pierre Ebel, Grenoble Cedex, France

Received 4 March 2003; accepted 22 May 2003

ABSTRACT

The photocycle in photoactive yellow protein (PYP) crystals was studied by single-crystal absorption spectroscopy with experimental setups for low-temperature and time-resolved measurements. Thin and flat PYP crystals, suitable for light absorption studies, were obtained using special crystallization conditions. Illumination of PYP crystals at 100 K led to the formation of a photostationary state, which includes at least one hypsochromic and one bathochromic photoproduct that resemble PYP_H and PYP_B, respectively. The effect of temperature, light color and light pulse duration on the occupancy of these low-temperature photoproducts was determined and appeared similar to that observed in solution. At room temperature a blueshifted photocycle intermediate was identified that corresponds to the blueshifted state of PYP (pB). Kinetic studies show that the decay of this blueshifted intermediate is biphasic at –12°C and 15-fold faster than that observed in solution at room temperature. These altered pB decay kinetics confirm a model that holds that the photocycle in crystals takes place in a shortcut version. In this version the key structural events of the photocycle, such as photoisomerization and reversible protonation of the chromophore, take place, but large conformational changes in the surrounding protein are limited by constraints imposed by the crystal lattice.

INTRODUCTION

Photoactive yellow protein (PYP) is a 125-residue bacterial photoreceptor protein that on light excitation of its covalently bound 4-hydroxy cinnamate chromophore enters a cyclic chain of reactions, the so-called photocycle (1). This photocycle has been extensively studied at room temperature as well as at low temperatures, leading to the identification of a number of spectroscopically distinct intermediates with an absorption maximum that is shifted relative to the absorbance maximum of the dark state of PYP (ground state of PYP, pG) at 446 nm. Illumination of a solution of PYP in a glycerol–water mixture cooled down to 77 K leads to the formation of a photostationary state containing at least two photoproducts: PYP_H or A₄₄₀ and PYP_B or A₄₉₀ (2,3). The partial occupancy of these intermediates depends strongly on the wavelength of illumination used.

Using time-resolved spectroscopy at room temperature, at least three transient ground-state intermediates have been identified: I₀ with a λ_{max} of 520 nm, I₁ or redshifted state of PYP (pR) with a λ_{max} of 465 nm and I₂ or blueshifted state of PYP (pB) with a λ_{max} of 355 nm (4–6). The structural basis for initiation of the photocycle is the *trans* to *cis* isomerization of the double bond of the chromophore (7–9), which leads to the subsequent formation of two redshifted intermediates on the pico- to nanosecond time scale. The redshifted intermediate pR is then converted on the sub-ms time scale to the long-lived intermediate pB. The latter is significantly blueshifted because of the protonation of the anionic chromophore, a process that has not been detected at low temperature (2,3). The last step in the photocycle is the decay of the blueshifted-state pB with the simultaneous recovery of the dark-state pG, involving reisomerization and deprotonation of the chromophore, which occurs on the sub-s time scale.

Structural changes associated with the formation and decay of optical intermediates have been analyzed in detail by a wide range of techniques, including X-ray crystallography (10–13), Fourier transform infrared (FTIR) spectroscopy (8,14,15) and nuclear magnetic resonance (NMR) spectroscopy (16). The application of time-resolved absorption spectroscopy under the same experimental conditions as those used for the application of these structural techniques is essential for a number of reasons. First, it allows monitoring of the presence of the optical intermediate of interest

¶Posted on the website on 5 June 2003

*To whom correspondence should be addressed at: Laboratory for Microbiology, Swammerdam Institute for Life Sciences, University of Amsterdam, Nieuwe Achtergracht 166, 1018WV Amsterdam, The Netherlands. Fax: 31-20-525-7056; e-mail: rkort@science.uva.nl

†This article is dedicated to the memory of my father Wil J. Kort, researcher in oncology at the Erasmus University, Rotterdam.

‡Current address: NIDDK, National Institutes of Health, Building 5, Bethesda, MD, USA.

Abbreviations: BR, bacteriorhodopsin; FTIR, Fourier transform infrared; FWHM, full width at half maximum; NMR, nuclear magnetic resonance; OD, optical density; pG, ground state of photoactive yellow protein, pR, redshifted state of photoactive yellow protein, pB, blueshifted state of photoactive yellow protein; PYP, photoactive yellow protein.

© 2003 American Society for Photobiology 0031-8655/03 \$5.00+0.00

and additional intermediates. Second, the experimental conditions to obtain the highest occupancy of the optical intermediate of interest can be established. Third, the reaction kinetics can be determined under the particular conditions needed for the various techniques, such as a thin protein film or a crystal, possibly at reduced hydration levels, extreme salt concentrations or extreme temperatures. Possible constraints on conformational changes due, for example, to low water content or intermolecular contacts in the crystal lattice can thus be identified.

Absorption measurements on PYP crystals appear much more difficult than in solution because their small dimensions and extremely high optical density in the blue region demand a very stable and well-focused monitoring light beam. In this study a home-built microspectrophotometer (17) was used to identify optically distinct photocycle intermediates in PYP crystals. Previous optical studies on PYP crystals in the hexagonal space group $P6_3$ suggested that the kinetic model for PYP in solution did not—although being quite similar—entirely match that of crystalline PYP. The alternative model, proposed to explain the PYP photocycle in crystals, included an additional blueshifted intermediate, on the basis of the observation that the recovery of the dark state was biphasic (18). However, the strong absorbance of PYP crystals in the region around 450 nm limited the spectral region for accurate optical measurements in these earlier studies (11,18). In this study we present a way to overcome this limitation by the preparation of very thin hexagons of PYP. In addition, we show the usefulness of single-crystal microspectrophotometry to identify photocycle intermediates in PYP in the crystalline state, and we report experimental conditions to obtain relatively high occupancies for these intermediates.

MATERIALS AND METHODS

Crystallization. PYP from *Halorhodospira halophila* strain BN9626 (previously known as *Ectothiorhodospira halophila*) was overproduced, reconstituted and purified as described (19,20). Crystals of space group $P6_5$ were obtained by the vapor diffusion method after 2–3 days of incubation at 20°C, with 25 mg/mL PYP and 40% (wt/vol) PEG2000 precipitant in 100 mM 2-(*N*-morpholino)-ethanesulphonic acid (MES), pH 6.5 as reported (21). Alternatively, $P6_5$ crystals with the same morphology and similar diffraction properties were obtained when PEG4000 was used as a precipitant. The latter crystals grew overnight. Crystals of space group $P6_3$ were grown at 20°C in 20 mM Na phosphate buffer, pH 7.0, and 2.55 M $(\text{NH}_4)_2\text{SO}_4$ as precipitant, according to the protocol described by McRee *et al.* (22).

X-ray diffraction. Diffracting properties of needles and flat crystals (symmetry $P6_5$) were analyzed at beamline station ID14-4 of the European Synchrotron Radiation Facility, Grenoble, France. Data were collected at 100 K with an X-ray wavelength of 0.939 Å using an ADSC Q4R detector.

Microspectrophotometer. The design of the absorption spectrophotometer was adapted from Hadfield and Hajdu (23). Spectra were recorded with the PC2000 2048-element linear charge-coupled device array fiber optic spectrometer (Ocean Optics Inc., Dunedin, FL). Monitoring light was focused on the crystal by two reflective objectives (focal spot diameter approximately 50 μm). The accessible wavelengths for absorption measurements ranged from about 200 to 850 nm. For a detailed description of this microspectrophotometer, see Bourgeois *et al.* (17).

Low-temperature spectroscopy. Excitation light was guided from a 75 W xenon light source to the crystal via a 225 μm fiber and a goniometer head with an adjustable fiber holder. Crystals were mounted with a cryoloop, directly from the mother liquor that contains 40% polyethylene glycol as a cryoprotectant. A 600 series Oxford Cryosystems nitrogen stream cooler controlled the temperature at the position of the sample. Temperatures given in this article are those set on the controller. To optimize the occupancy of the bathochromically shifted low-temperature photoproduct, conditions were used as indicated below, unless specified otherwise: light color, actinic blue light, selected by a broadband interference filter (maximum transmission at 400 nm; full width at half maximum [FWHM] = 80 nm) from the

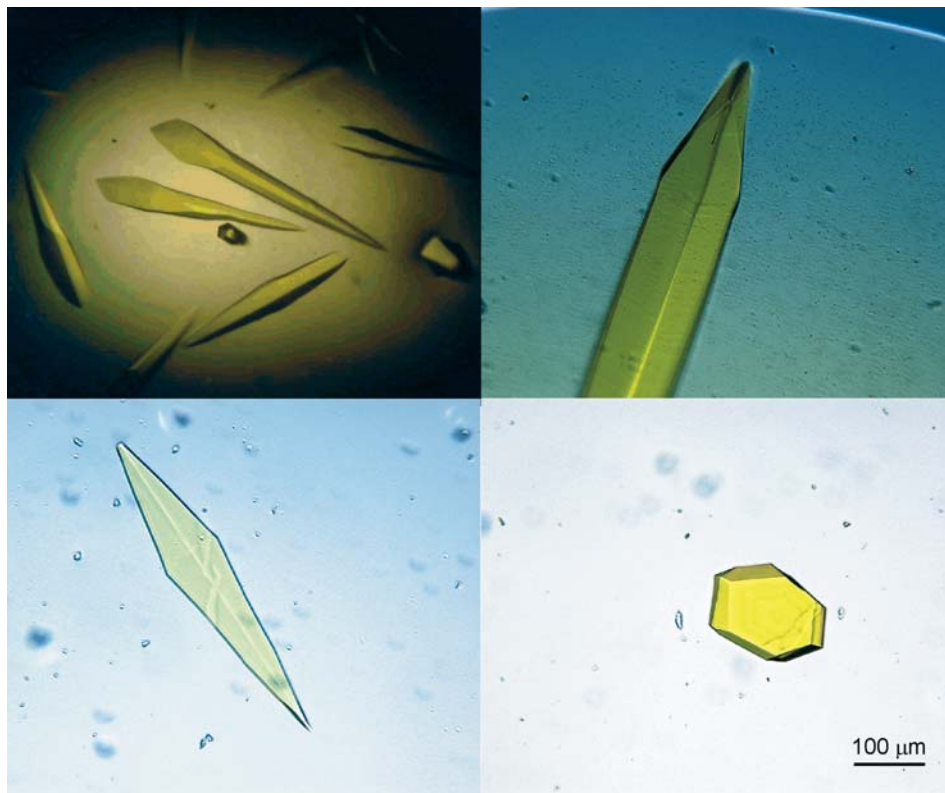


Figure 1. Selection of $P6_5$ crystals used in this study. Top left: Typical crystal shape of $P6_5$ PYP crystals grown at 20°C in a hanging drop with a precipitant solution of 40% (wt/vol) PEG2000 and 100 mM MES, pH 6.5. Top right: Single $P6_5$ PYP crystal grown in a hanging drop. Bottom left: Flat needle grown in a protein-precipitant film. Bottom right: Flat hexagon grown in a protein-precipitant film. Bar indicates the scale of the three single-crystal pictures.

xenon light source; light pulse duration, 60 s; temperature, 100 K. Spectra were measured using a continuous xenon light source (Fig. 2) or by averaging 10 spectra monitored with a 1.3 μs FWHM pulse from a xenon flash lamp (Oriel Inc., Stratford, CT; 50 mJ) (Fig. 3) to avoid formation of photocycle intermediates by the monitoring light.

Time-resolved spectroscopy. For the room temperature (22°C) experiment with 2.5 ms time resolution, PYP crystals were mounted in a 0.7 mm glass capillary. Decay of the pB intermediate ($\lambda_{\text{max}} = 355 \text{ nm}$) was measured as a function of pump-probe delay time (Fig. 4A). The crystal was excited with a 0.5 ms FWHM xenon flash lamp, in combination with a 435 nm long-pass filter. Spectra were measured with a xenon flash lamp (1.3 μs FWHM) and 10 spectra were average. The excitation light, monitoring light and spectrophotometer were synchronized with a pulse generator model DG535 (Stanford Research Systems Inc., Sunnyvale, CA).

For the time-resolved experiment with ~ 320 ms time resolution (Fig. 4B), the temperature was lowered to -12°C to decelerate the rate of recovery of the ground state of PYP. Excitation of crystalline PYP was performed with a shutter-controlled 488 nm laser pulse of 1 s duration from an argon ion laser (Melles Griot, Carlsbad, CA). Light was guided to the reflective objective by a 600 μm diameter optical fiber. The radius of the focused laser spot was 90 μm . Spectra were measured with a xenon light source using an integration time of 3 ms per spectrum, and 10 spectra were averaged per time point. Crystals were mounted in a cryoloop and protected from dehydration by soaking in paraffin oil (Hampton Research, Laguna Niguel, CA). The laser power at the sample position was 0.55 mW, as determined through a pinhole of 25 μm radius.

The time-resolved experiment with ~ 25 ms time resolution was carried out using the same experimental setup and monitoring light source used for the 300 ms resolution experiment, but instead of a full spectrum, five time channels were measured with a bandwidth of three pixels. The integration time was 3 ms per spectrum, and two spectra were averaged per time point. The formation and decay of the blueshifted intermediate was monitored at 350 and 360 nm, whereas the ground-state bleach was monitored at 450 and 460 nm. As a reference, measurements were performed at 600 nm.

RESULTS

Control of crystal morphology. The size of the $P6_5$ crystals of PYP ranged from $240 \times 40 \times 40 \mu\text{m}^3$ to $1200 \times 200 \times 200 \mu\text{m}^3$ (Fig. 1; top left). In the hexagonal PYP crystals of unit cell dimensions, $a = b = 40 \text{ \AA}$ and $c = 118 \text{ \AA}$ (21), and the protein concentration equals 61 mM. On the basis of the molar extinction coefficient of $\epsilon_{446} = 45\,500 \text{ M}^{-1} \text{ cm}^{-1}$ (24), this implies a linear absorption coefficient at the absorption maximum μ_{446} of $0.28 \mu\text{m}^{-1}$, assuming that the PYP transition dipole moments are randomly oriented in the crystal. The $P6_5$ crystals show very similar absorption coefficient compared with $P6_3$ crystals, for which a value of $0.25 \mu\text{m}^{-1}$ was calculated (11). Thus theoretically, a crystal of approximately 3.6 μm thickness will display an optical density (OD) of 1 at 446 nm. Accordingly, the OD values at the absorption maximum in the $P6_5$ PYP crystals range from 11 to 55, which is far too high to reliably monitor absorption changes. However, by controlling the morphology of these crystals—through the use of a thin protein-precipitant film instead of a drop—we were able to obtain thin crystals with a relatively large surface area (Fig. 1; bottom left and right). The film was made with 2–4 μL of the protein-precipitant solution spread over a cover glass to a surface area of approximately 30 mm^2 . This led to the formation of flat needles (size $100 \times 16 \times 16 \mu\text{m}^3$ to $600 \times 100 \times 100 \mu\text{m}^3$) and hexagons (size $50 \times 50 \times 8 \mu\text{m}^3$ to $300 \times 300 \times 50 \mu\text{m}^3$). The calculated OD₄₄₆ values of the latter flat type of crystals vary between 2 and 14. In our measurements, however, the OD values of many of these crystals appeared significantly lower, between 1 and 2 at the absorption maximum (Figs. 2–5), because the absorption is dependent on the orientation of the crystal in the monitoring light beam (18). Thus, the use of the thin protein-precipitant film for PYP crystallization led to sufficiently flat crystals for reliable spectroscopic measurements. Alternatively,

spectra could be recorded after focusing the monitoring light on the tip of a needle-type crystal (Fig. 1; top right), provided that the local optical density at 446 nm is within the range of 1–2.

X-ray diffraction. Diffraction patterns were collected at 100 K on both forms of $P6_5$ PYP crystals as shown in Fig. 1, bottom left and right. The unit cell dimensions were refined to $a = b = 40.20 \text{ \AA}$ and $c = 118.01 \text{ \AA}$, slightly smaller than the dimensions $a = b = 40.56 \text{ \AA}$ and $c = 118.09 \text{ \AA}$ reported previously (21). The relatively thick crystals with the needle morphology diffracted to a higher resolution of 1.1 \AA than the flat hexagons, which diffracted only down to 2 \AA .

Low-temperature microspectrophotometry. The absorption spectrum of the ground state of crystalline PYP at 100 K shows characteristics similar to those observed for PYP in an amorphous glycerol solution. Its absorbance maximum is slightly redshifted from 446 to 448 nm, the absorbance band is narrowed and a shoulder appears at the high-energy side of the band as a result of the vibrational fine structure (2,3). Excitation of a PYP crystal at 100 K with blue light of $400 \pm 40 \text{ nm}$ led to a significant decrease of the 448 nm absorption band. In addition, a slight blueshift occurred in the spectrum from 448 to 443 nm, and a shoulder was formed with a maximum at approximately 490 nm (Fig. 2). The latter absorption increase is due to the accumulation of a bathochromic low-temperature photoproduct previously assigned to PYP_B (2). This intermediate may correspond to the early, redshifted, room temperature photocycle intermediate I₀ (4). The observed residual absorption band at 490 nm in the reference spectrum in Fig. 2 results from the formation of PYP_B in the crystal by the continuous xenon monitoring light source. In addition to the increase in absorption at 490 nm, the dashed absorption spectrum in Fig. 2 shows a slight shift of the main absorption maximum to a shorter wavelength, indicating the formation of a second low-temperature intermediate, with a slightly blueshifted absorption band. Such an intermediate has been previously identified in amorphous glycerol solution as PYP_H, with a maximal absorption at 442 nm (2), whereas a fluorescent species can be formed on prolonged illumination with an absorbance maximum at 430 nm (3).

To further optimize the yield of these low-temperature intermediates, the following conditions were varied: (1) light color; (2) temperature; and (3) length of the actinic blue light pulse. Crystals were illuminated for 60 s with the same xenon light source and four selected optical filters. The use of a 440 nm broadband filter (FWHM, 100 nm), a 410 nm narrowband (FWHM, 10 nm) or a 435 nm long-pass filter led to a relative increase at OD₄₉₀ of 27%, 60% and 6%, respectively, compared with that obtained with the 400 nm broadband filter with FWHM = 80 nm (data not shown). In this experiment it was not possible to normalize the spectra accurately because the interruption of the nitrogen cryostream for thermal relaxation of the low-temperature products formed causes slight variations in crystal position. However, it is evident that a blueshifted and a redshifted intermediate are formed in a ratio that depends on the light color used. As expected, yellow light ($>435 \text{ nm}$) leads to the lowest PYP_B occupancy and highest PYP_H occupancy, whereas blue light of $400 \pm 40 \text{ nm}$ leads to the inverse effect. This can be explained by the notion that the formation of PYP_H and PYP_B is photoreversible, and thus these intermediates will be partially converted back to the dark state when their absorption bands at 442 and 490 nm, respectively, are excited. Besides light color, light intensity also plays a role. The difference in PYP_B occupancy obtained using the $410 \pm 5 \text{ nm}$ filter and the $400 \pm 40 \text{ nm}$ filter can be explained by the fact that the narrow-

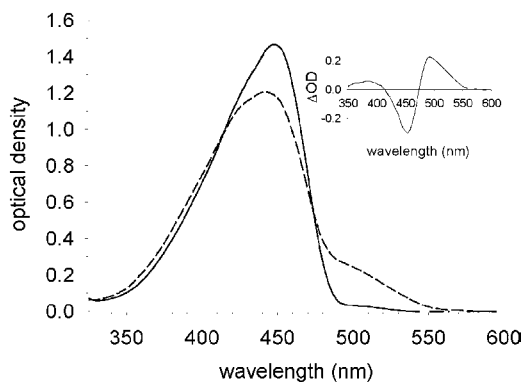


Figure 2. Blue light-induced absorption changes in a single $P6_5$ PYP crystal at 100 K. The solid line indicates the reference absorption spectrum of a single $P6_5$ crystal at 100 K. The dashed line indicates the absorption spectrum of the same crystal illuminated with blue light of 400 ± 40 nm for a period of 60 s at 100 K. The inset shows the difference spectrum between the absorption spectrum of the blue light-illuminated crystal and the reference absorption spectrum. Spectra were monitored with the continuous xenon light source.

band filter transmits a relatively low light intensity that probably does not penetrate through the entire crystal.

In Fig. 3A the formation of PYP_B in crystalline PYP is presented as a function of temperature. After exposure of a PYP crystal for 60 s to blue light of 400 ± 40 nm, the highest occupancy of PYP_B was observed at 90 K, whereas at temperatures higher than 130 K, hardly any PYP_B could be detected. To ensure that 60 s of light exposure was sufficient to form the maximal amount of PYP_B with the current crystal thickness and light intensity, spectra were also collected as a function of the exposure time (Fig. 3B). To repopulate the ground-state pG after each measurement, the temperature was raised to 293 K by blocking the cold nitrogen stream for several seconds. Subsequently, the crystal was refrozen to 100 K. An exponential fit of the relative increase at OD_{490} as a function of the light exposure time resulted in a rise time of 0.4 s. It should be noted that this rise time is not identical to that for PYP_B formation because a relatively long light pulse is used and reverse photochemistry is involved. Finally, the thermal decay of PYP_B in the dark was investigated at 100 K (Fig. 3C). The derived decay time equals 100 s at 100 K. Under the conditions used the OD_{490} recovered to approximately 40% of the initial value, indicating the involvement of a second, slower component.

Time-resolved microspectrophotometry. For time-resolved experiments PYP crystals were mounted in capillaries at 22°C and exposed to millisecond light flashes, which preceded a microsecond monitoring light flash by delays ranging from 2.5 to 100 ms (Fig. 4A). At 2.5 ms delay after the actinic flash, the absorption increased in the spectral range from 300 to 420 nm, whereas a slight decrease was observed of the 449 nm absorption band. The absorption in the 300–420 nm region decays with a characteristic time of about 10 ms, as indicated in the inset of Fig. 4A, in which the OD_{355} is plotted *versus* time. After 100 ms delay the absorption spectrum basically matches that of the crystal before the flash, indicating the absence of slower components in the recovery reaction. The spectra show an isosbestic point at 418 nm.

Subsequently, a thin $P6_3$ PYP crystal was placed in a cryoloop, and spectra were monitored at -12°C every 320 ms, before, during and after a shutter-controlled 1 s exposure to 488 nm laser light (Fig. 4B). Exposure of the crystal to the 488 nm blue laser light clearly resulted in bleaching of the main absorption band of PYP,

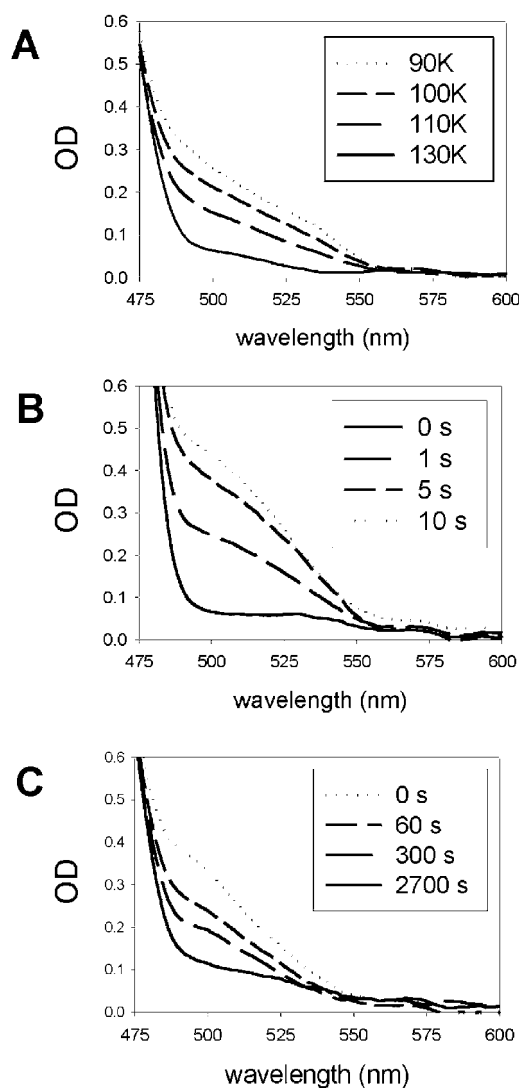


Figure 3. Effect of variation of temperature (A), period of actinic illumination (B) and dark relaxation (C) on the occupancy of PYP_B in $P6_5$ PYP crystals. Crystals were illuminated with blue light of 400 ± 40 nm for a period of 60 s at 100 K, unless specified otherwise. A: Temperature was varied in the range from 90 to 130 K via the nitrogen cryostream controller. B: Pulse duration of actinic blue light was varied from 0 to 10 s. C: Time interval of spontaneous PYP_B relaxation was varied in the absence of actinic light. Spectra were obtained by averaging 10 traces monitored with a $1.3 \mu\text{s}$ FWHM pulse of a xenon flash lamp.

whereas an additional, blueshifted band appeared in the region between 300 and 420 nm. The apparent negative absorption around 488 nm results from stray light from the laser. The apparently increasing absorbance, when going from 750 to 520 nm, results from scattering by the sample, which is stronger at shorter wavelengths. This is in agreement with the high OD value of the sample at 330 nm, which is close to zero in the absence of scattering. The recovery of the ground-state absorption band in the inset of Fig. 4B shows a rise time of 300 ms. The isosbestic point of the transition is at 404 nm. Even at 3 s after the laser pulse, full recovery of the ground state is not observed, suggesting that this recovery is multiexponential. The experiment was repeated with $P6_5$ crystals of similar dimensions, and no significant differences in spectral changes and kinetics were observed (data not shown).

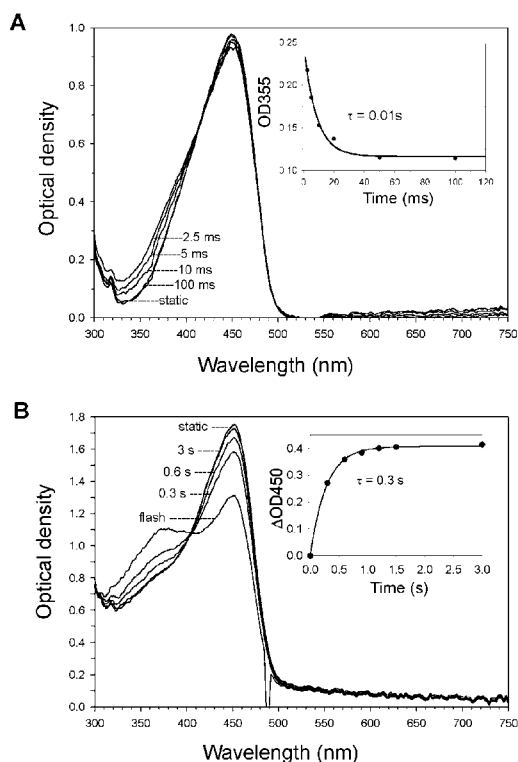


Figure 4. Analysis of the dynamics of relaxation of the pB intermediate in single PYP crystals. A: pB relaxation was measured at room temperature with millisecond time resolution on a $P6_5$ crystal mounted in a glass capillary in the presence of a drop of mother liquor. The crystal was excited with a 0.5 ms FWHM xenon flash lamp, in combination with a 435 nm long-pass filter. B: Measurement at -12°C with 0.3 s time resolution on a $P6_3$ crystal soaked in paraffin oil. The crystal was excited with the 488 nm line of a CW argon ion laser for a period of 1 s.

To improve the time resolution to ~ 25 ms in the next series of measurements, five wavelengths, instead of full spectra, were recorded in parallel. In Fig. 5 the trace recorded at OD_{350} before, during and after the 1 s laser pulse of 488 nm is presented. For a proper fit a biexponential function has to be assumed, as can be judged from the residuals of the fits. The estimated relaxation rates are 0.78 and 0.25 s, with relative amplitudes of 70% and 30%, respectively. The observed biphasic decay of pB from the photostationary state to the stable dark state (pG) is in agreement with previous measurements on PYP crystals (18).

DISCUSSION

The procedure reported in this article to adjust crystallization conditions such that flat hexagons are formed may become important for light-sensitive proteins in general. It is recognized more and more that structural studies on transient intermediates should be paralleled by optical studies to characterize the mixture of intermediates present (25–27). The flat and thin PYP hexagons form a very attractive material to reach this goal because they are sufficiently transparent to allow absorption spectroscopy. This approach may restrict the diffracting volume of the crystals. However, for optical studies during the X-ray diffraction experiment, a perpendicular arrangement of the X-ray and light beams may be the optimal experimental setup for simultaneous data collection on the flat hexagonal crystals. In this case, one needs to find the optimal thickness for the crystal that minimally compromises on

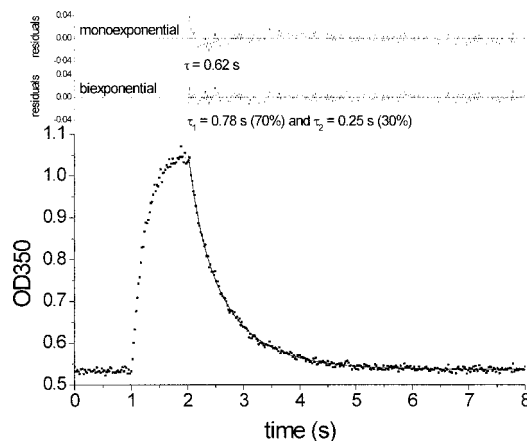


Figure 5. Kinetic analysis of the relaxation of the pB state of PYP in a single crystal at -12°C . A $P6_3$ crystal was mounted in a cryoloop after soaking in paraffin oil. It was illuminated with the 488 nm laser line of a CW argon ion laser for a period of 1 s. The optical density at 350 nm has been plotted against time. A biexponential fit is represented as the full line from 2 to 8 s. The residuals show the increase in the quality of the biexponential over the monoexponential fit.

diffracting volume on the one hand and transparency on the other.

The exposure of a PYP crystal to blue light of 400 ± 40 nm at 100 K leads to the formation of a photostationary state of intermediates that includes at least the bathochromic intermediate PYP_B and the hypsochromic intermediate PYP_H (Fig. 2). No significant differences have been observed between the optical studies on crystals described in this study and those on amorphous glycerol solution (2) with respect to the formation of this photostationary state or PYP_B behavior as presented in Fig. 3. Apparently, the light-induced formation of photoproducts at very low temperatures, often referred to as early intermediates (11), is not affected by the crystal lattice. Comparisons of the low-temperature studies on PYP crystals described in this study with those carried out on the photoisomerizable photoreceptor protein bacteriorhodopsin (BR) under similar conditions led to the identification of a number of striking similarities and differences. In the case of BR the K intermediate can be considered as the equivalent of PYP_B . This is the first photoproduct of the photocycle of BR that can be stabilized at liquid nitrogen temperatures, and its formation is accompanied by a 40 nm redshift from 578 to 608 nm. In contrast to PYP_B , K is formed with a high quantum yield even at 4 K and is stable in the dark up to 130 K (28). It is obvious from the absorption spectra in Fig. 2 that only a relatively small fraction of the dark state of PYP can be converted to PYP_B under the experimental conditions used. A maximal occupancy of approximately 20% for PYP_B can be calculated from the relative depletion of the absorption band originating from the ground state of PYP, whereas at least 50% of BR can be converted to K at 100 K (29). Possibly, the much lower efficiency for the PYP to PYP_B conversion results from the simultaneous formation of the blueshifted intermediate PYP_H , a side reaction that has not been observed in the BR low-temperature photocycle. Another striking difference is the instability of PYP_B even at 100 K, as presented in Fig. 3C. The majority of PYP in the redshifted PYP_B state decays in the dark at 100 K with a time constant of approximately 100 s, presumably to PYP_{BL} (2), whereas part of PYP_B is trapped for much longer time periods. An increase in the temperature by

blocking the nitrogen cryostream led to the disappearance of the residual absorption band at 490 nm. This complicated behavior of PYP_B at low temperature may indicate the presence of a mixture of low-temperature species with similar, redshifted absorption spectra. However, further decrease to liquid helium temperatures (4–9 K) did not resolve this point because, in contrast to the situation in BR (30), photochemical reactions were not observed at those temperatures in PYP (Ravelli *et al.*, unpublished; Van der Horst, Premvardhan *et al.*, unpublished).

The stability of low-temperature intermediates is of utmost importance for the structural characterization of these intermediates by X-ray diffraction studies that require relatively long exposure times. One way to overcome the decrease in occupancy of intermediates resulting from thermal decay is the use of continuous actinic illumination during data collection, as has been applied in the case of the elucidation of the structure of the low-temperature intermediate, which was tentatively assigned to PYP_{BL} (11). PYP_{BL}, the thermal relaxation product of PYP_B, could not be unambiguously identified in our studies (Fig. 3A). It was extremely difficult to deconvolute the three low-temperature species, PYP_H, PYP_{HL} and PYP_{BL}, in the single-crystal absorption spectra obtained with our experimental setup because very subtle absorption changes resulted from small displacements of the crystal during the experiment. The low-temperature intermediates all have slightly blueshifted absorption bands that overlap with the dark-state absorption band of PYP. Furthermore, it is relevant to note that the trapped intermediates of photoactive proteins are photoactive themselves. Thus, continuous illumination of these crystals increases the risk of formation of secondary photoproducts.

At room temperature, pB decays rapidly in the crystal with a time constant of 10 ms, as presented for the time-resolved experiment in Fig. 4A. This is 15-fold faster than in solution, where this time constant has been determined to 150 ms (5,6). It should be noted that the recovery reaction for pG is strongly pH dependent. The rate constant for this reaction as a function of pH from 5 to 10 is a bell-shaped curve with a maximally 16-fold change and a maximum at pH 7.9 (31). The inclusion of this pH effect makes the difference in time constants for the pG recovery reaction in solution and a crystal even larger because the time constant is approximately 300 ms in solution at pH 6.5 of the actual crystallization condition (31). The use of paraffin oil to prevent dehydration of the crystal for the experiments presented in Figs. 4B and 5 and the presence of the crystallization mother liquor will also slightly affect the photocycle kinetics. This cannot explain the observed differences between solution and crystal because increased viscosity and hydrophobicity of the medium decrease the pG recovery rate (5,24), the opposite effect of what has been observed in this study. However, effects of the mother liquor on the photocycle in the crystal cannot be explained easily because the content in the solvent channels in the crystal is not necessarily identical to that of the bulk of the mother liquor.

The results presented in this study indicate that PYP goes through a genuine photocycle, involving an initial isomerization and a subsequent protonation of the chromophore. The decay of pB is well described in crystals at -12°C with a biexponential function with time constants of $\tau = 0.78$ s (70%) and $\tau = 0.25$ s (30%; Fig. 5). Previous studies with transient absorption spectroscopy on PYP crystals showed faster biexponential decay for pB, as expected at the higher temperature of -4°C , with time constants of $\tau = 0.71$ s (60%) and $\tau = 0.19$ s (40%), respectively (18). Also flash-induced absorption changes in solution indicated a biphasic decay with rate

constants of $\tau = 0.15$ s (93%) and $\tau = 2.0$ s (7%) at 20°C (6). These results may indicate parallel pathways in the photocycle of PYP, for which it will be challenging to resolve the associated structural changes.

The fast pB decay kinetics suggest that the protein goes through a shortcut version of the photocycle in the crystal. FTIR studies indicate that light-induced structural changes in the protein backbone associated with pG recovery are dramatically reduced in PYP crystals (15). In addition, the point was raised that partial dehydration of the protein in the crystal probably contributes to the suppression of large structural changes on pB formation. This is in agreement with the findings in this study and recent observations, indicating fast pB decay kinetics in partially dehydrated PYP films (Van der Horst *et al.*, unpublished). In addition, conformational changes may not occur to the same extent as in solution because they could be limited by intermolecular contacts in the crystal lattice. This is in line with the concept of PYP being a photoreceptor protein with a rigid core surrounded by a soft body, in which small light-induced changes in the chromophore configuration lead to large changes in protein conformation (32). The latter changes and the rate at which they occur are—in contrast to changes in the rigid core—easily affected by their environment.

The results presented in this study suggest that the low-temperature photocycle and thus probably also the early photocycle intermediates, involving relatively small-amplitude structural changes, can be accurately determined by crystallographic techniques. The altered photocycle kinetics in crystals indicates that for the description of conformational changes of larger amplitude on the millisecond to second time scale, independent evidence by complementary techniques using PYP in concentrated solution, such as FTIR spectroscopy and NMR spectroscopy, is important. However, highly concentrated protein solutions do not indisputably reflect the *in vivo* situation, where a downstream signaling partner may affect the photochemical reactions of the photoreceptor protein (33).

Acknowledgement—The authors are very grateful to Dr. Keith Moffat for valuable suggestions.

REFERENCES

- Hellingwerf, K. J. (2000) Key issues in the photochemistry and signalling-state formation of photosensor proteins. *J. Photochem. Photobiol. B: Biol.* **54**, 94–102.
- Imamoto, Y., M. Kataoka and F. Tokunaga (1996) Photoreaction cycle of photoactive yellow protein from *Ectothiorhodospira halophila* studied by low-temperature spectroscopy. *Biochemistry* **35**, 14047–14053.
- Hoff, W. D., S. L. S. Kwa, R. Van Grondelle and K. J. Hellingwerf (1992) Low temperature absorbance and fluorescence spectroscopy of the photoactive yellow protein from *Ectothiorhodospira halophila*. *Photochem. Photobiol.* **56**, 529–539.
- Ujj, L., S. Devanathan, T. E. Meyer, M. A. Cusanovich, G. Tollin and G. H. Atkinson (1998) New photocycle intermediates in the photoactive yellow protein from *Ectothiorhodospira halophila*: picosecond transient absorption spectroscopy. *Biophys. J.* **75**, 406–412.
- Meyer, T. E., E. Yakali, M. A. Cusanovich and G. Tollin (1987) Properties of a water-soluble, yellow protein isolated from a halophilic phototrophic bacterium that has photochemical activity analogous to sensory rhodopsin. *Biochemistry* **26**, 418–423.
- Hoff, W. D., I. H. van Stokkum, H. J. van Ramesdonk, M. E. van Brederode, A. M. Brouwer, J. C. Fitch, T. E. Meyer, R. van Grondelle and K. J. Hellingwerf (1994) Measurement and global analysis of the absorbance changes in the photocycle of the photoactive yellow protein from *Ectothiorhodospira halophila*. *Biophys. J.* **67**, 1691–1705.
- Kort, R., H. Vonk, X. Xu, W. D. Hoff, W. Crielaard and K. J. Hellingwerf (1996) Evidence for *trans-cis* isomerization of the *p*-coumaric

- acid chromophore as the photochemical basis of the photocycle of photoactive yellow protein. *FEBS Lett.* **382**, 73–78.
8. Imamoto, Y., Y. Shirahige, F. Tokunaga, T. Kinoshita, K. Yoshihara and M. Kataoka (2001) Low-temperature Fourier transform infrared spectroscopy of photoactive yellow protein. *Biochemistry* **40**, 8997–9004.
 9. Gensch, T., C. C. Gradinaru, I. H. M. van Stokkum, J. Hendriks, K. J. Hellingwerf and R. van Grondelle (2002) The primary photoreaction of photoactive yellow protein (PYP): anisotropy changes and excitation wavelength dependence. *Chem. Phys. Lett.* **356**, 347–354.
 10. Genick, U. K., G. E. O. Borgstahl, K. Ng, Z. Ren, C. Pradervand, P. M. Burke, V. Srajer, T. Y. Teng, W. Schildkamp, D. E. McRee, K. Moffat and E. D. Getzoff (1997) Structure of a protein photocycle intermediate by millisecond time-resolved crystallography. *Science* **275**, 1471–1475.
 11. Genick, U. K., S. M. Soltis, P. Kuhn, I. L. Canestrelli and E. D. Getzoff (1998) Structure at 0.85 Å resolution of an early protein photocycle intermediate. *Nature* **392**, 206–209.
 12. Perman, B., V. Srajer, Z. Ren, T. Y. Teng, C. Pradervand, T. Ursby, D. Bourgeois, F. Schotte, M. Wulff, R. Kort, K. Hellingwerf and K. Moffat (1998) Energy transduction on the nanosecond time scale: early structural events in a xanthopsin photocycle. *Science* **279**, 1946–1950.
 13. Ren, Z., B. Perman, V. Srajer, T. Y. Teng, C. Pradervand, D. Bourgeois, F. Schotte, T. Ursby, R. Kort, M. Wulff and K. Moffat (2001) A molecular movie at 1.8 Å resolution displays the photocycle of photoactive yellow protein, a eubacterial blue-light receptor, from nanoseconds to seconds. *Biochemistry* **40**, 13788–13801.
 14. Brudler, R., R. Rammelsberg, T. T. Woo, E. D. Getzoff and K. Gerwert (2001) Structure of the I-1 early intermediate of photoactive yellow protein by FTIR spectroscopy. *Nat. Struct. Biol.* **8**, 265–270.
 15. Xie, A. H., L. Kelemen, J. Hendriks, B. J. White, K. J. Hellingwerf and W. D. Hoff (2001) Formation of a new buried charge drives a large-amplitude protein quake in photoreceptor activation. *Biochemistry* **40**, 1510–1517.
 16. Rubinstenn, G., G. W. Vuister, F. A. Mulder, P. E. Dux, R. Boelens, K. J. Hellingwerf and R. Kaptein (1998) Structural and dynamic changes of photoactive yellow protein during its photocycle in solution. *Nat. Struct. Biol.* **5**, 568–570.
 17. Bourgeois, D., X. Vernede, V. Adam, E. Fioravanti and T. Ursby (2002) A microspectrophotometer for UV-visible absorption and fluorescence studies of protein crystals. *J. Appl. Crystallogr.* **35**, 319–326.
 18. Ng, K., E. D. Getzoff and K. Moffat (1995) Optical studies of a bacterial photoreceptor protein, photoactive yellow protein, in single crystals. *Biochemistry* **34**, 879–890.
 19. Imamoto, Y., T. Ito, M. Kataoka and F. Tokunaga (1995) Reconstitution photoactive yellow protein from apoprotein and p-coumaric acid derivatives. *FEBS Lett.* **374**, 157–160.
 20. Kort, R., W. D. Hoff, M. Van West, A. R. Kroon, S. M. Höffer, K. H. Vlieg, W. Crielaand, J. J. Van Beeumen and K. J. Hellingwerf (1996) The xanthopsins: a new family of eubacterial blue-light photoreceptors. *EMBO J.* **15**, 3209–3218.
 21. van Aalten, D. M. F., W. Crielaand, K. J. Hellingwerf and L. Joshua-Tor (2000) Conformational substates in different crystal forms of photoactive yellow protein—correlation with theoretical and experimental flexibility. *Protein Sci.* **9**, 64–72.
 22. McRee, D. E., T. E. Meyer, M. A. Cusanovich, H. E. Parge and E. D. Getzoff (1986) Crystallographic characterization of a photoactive yellow protein with photochemistry similar to sensory rhodopsin. *J. Biol. Chem.* **261**, 13850–13851.
 23. Hadfield, A. and J. Hajdu (1993) A fast and portable microspectrophotometer for protein crystallography. *J. Appl. Crystallogr.* **26**, 839–842.
 24. Meyer, T. E., G. Tollin, J. H. Hazzard and M. A. Cusanovich (1989) Photoactive yellow protein from the purple phototrophic bacterium, *Ectothiorhodospira halophila*. Quantum yield of photobleaching and effects of temperature, alcohols, glycerol, and sucrose on kinetics of photobleaching and recovery. *Biophys. J.* **56**, 559–564.
 25. Royant, A., K. Edman, T. Ursby, E. Pebay-Peyroula, E. M. Landau and R. Neutze (2000) Helix deformation is coupled to vectorial proton transport in the photocycle of bacteriorhodopsin. *Nature* **406**, 645–648.
 26. Royant, A., K. Edman, T. Ursby, E. Pebay-Peyroula, E. M. Landau and R. Neutze (2001) Spectroscopic characterization of bacteriorhodopsin's L-intermediate in 3D crystals cooled to 170 K. *Photochem. Photobiol.* **74**, 794–804.
 27. Heberle, J., G. Buldt, E. Koglin, J. P. Rosenbusch and E. M. Landau (1998) Assessing the functionality of a membrane protein in a three-dimensional crystal. *J. Mol. Biol.* **281**, 587–592.
 28. Balashov, S. P. and T. G. Ebrey (2001) Trapping and spectroscopic identification of the photointermediates of bacteriorhodopsin at low temperatures. *Photochem. Photobiol.* **73**, 453–462.
 29. Xie, A. H. (1990) Quantum efficiencies of bacteriorhodopsin photochemical reactions. *Biophys. J.* **58**, 1127–1132.
 30. Iwasa, T., F. Tokunaga and T. Yoshizawa (1979) Photoreaction of *trans*-bacteriorhodopsin at liquid helium temperature. *FEBS Lett.* **101**, 121–124.
 31. Genick, U. K., S. Devanathan, T. E. Meyer, I. L. Canestrelli, E. Williams, M. A. Cusanovich, G. Tollin and E. D. Getzoff (1997) Active site mutants implicate key residues for control of color and light cycle kinetics of photoactive yellow protein. *Biochemistry* **36**, 8–14.
 32. Reat, V., H. Patzelt, M. Ferrand, C. Pfister, D. Oesterheld and G. Zaccari (1998) Dynamics of different functional parts of bacteriorhodopsin: H-2H labeling and neutron scattering. *Proc. Natl. Acad. Sci. USA* **95**, 4970–4975.
 33. Spudich, E. N. and J. L. Spudich (1993) The photochemical reactions of sensory rhodopsin I are altered by its transducer. *J. Biol. Chem.* **268**, 16095–16097.